Title
Three-dimensional comparison of asymmetry in different sagittal skeletal patterns using geometric morphometrics

Permalink
https://escholarship.org/uc/item/6jd2g0z2

Author
Nguyen, Emerald

Publication Date
2014

Peer reviewed|Thesis/dissertation

Three-dimensional Comparison of Asymmetry in Different Sagittal Skeletal Patterns using

Geometric Morphometrics

Emerald Nguyen,DDS

THESIS

Submitted in partial satisfaction of the requirements for the degree of

MASTER OF SCIENCE

in

Oral and Craniofacial Sciences

in the

GRADUATE DIVISION

of the

UNIVERSITY OF CALIFORNIA, SAN FRANCISCO

DEDICATION

I would like to dedicate this thesis to my family for their unconditional love and support. You have provided me with every means to succeed and have been my foundation that has allowed me to progress and achieve my goals while keeping myself emotionally and physically grounded. I could not be where I am today without all of you.

ACKNOWLEDGEMENTS

Three-dimensional Comparison of Asymmetry in Different Sagittal Skeletal Patterns using Geometric Morphometrics

Emerald Nguyen, DDS

ABSTRACT

Objective: To compare the difference in type and quantity of asymmetry between Class I, Class II, and Class III sagittal skeletal patterns using geometric morphometrics.

Methods: Surface models were constructed from pre-treatment three-dimensional CBCT scans of 144 patients (41 males, 103 females) randomly selected from the database at the University of California, San Francisco, Division of Orthodontics. There were a total of 62 skeletal Class I (0≤ANB≤4), 63 skeletal Class II (ANB>4), and 19 skeletal Class III (ANB<0) subjects. The surface models were constructed using Amira software (Mercury Computer Systems GmbH, Berlin, Germany)) for optimal viewing of various structures, including the maxilla, zygomatic arches, condyles, and mandibular body. Landmark placement (n=183) was completed using Landmark software (Institute for Data Analysis and Visualization (IDAV), UCDavis). Landmarks were identified for each individual and after Procrustes superimposition of the raw coordinates and deviations from bilateral symmetry were analyzed by Principal Components Analysis (PCA).

Results: Permutation tests of the Procrustes distance showed that there was a statistically significant difference between Class I and Class III groups and between the Class II and Class III groups, but no difference between Class I and Class II groups. Principal component 1 (PC1) was significant for anterior mandibular deviations to the left with compensation of the remaining craniofacial structures. The average PC1 score for the Class III group was significantly different

than that of the Class I and Class II groups. Hartigan's dip test showed that asymmetries within Class III population may have a bimodal distribution with a predilection for left side deviations.

Conclusions: Asymmetries are more likely seen in skeletal Class III patients than in Class I and Class II patients. This asymmetry tends to be localized in the anterior mandible and is more often deviated to the left than right side.

TABLE OF CONTENTS

LIST OF TABLES

LIST OF FIGURES

INTRODUCTION

Proper diagnosis is essential for ensuring a successful outcome of any applied therapy, including orthodontics and orthognathic surgery. Clinicians have long acknowledged that the clinical significance of structural facial asymmetries lies in the fact that the orthodontist is limited to dental manipulation and that structural facial symmetries are not amenable to change by orthodontic means (Fischer 1954). However, a misdiagnosis of facial asymmetry can result in the wrong treatment plan for a patient. Therefore, accurate evaluations of facial asymmetry are crucial in orthodontic practice. Diagnosis has traditionally been based on planar two-dimensional (2D) radiographs, but new technology now offers three-dimensional (3D) volumetric images. This technology may improve the clinician's ability to identify, diagnose, quantify, and subsequently treat patient asymmetries (Cattaneo *et al.* 2008). However, at this time, there is a lack of a means of easily quantifying these 3D images. This study aims to compare the difference in type and quantity of asymmetry among Class I, Class II, and Class III sagittal skeletal patterns using 3D imaging and landmarked-based geometric morphometrics.

Defining Asymmetry

Symmetry is defined as the correspondence in size, form, and arrangement of parts on opposite sides of a plane, line, or point; in other words, symmetry means balance (Fischer 1954). There are primarily three kinds of asymmetry that are recognized (Graham et *al.* 1993): fluctuating asymmetry, directional asymmetry, and antisymmetry.

Fluctuating asymmetry consists of 'minor, nondirectional deviations from bilateral symmetry (Palmer and Strobeck, 1986).' Researchers have offered various explanations the

1

developmental origins of fluctuating asymmetry (Graham et *al.*1993, Palmer and Strobeck, 1992). Some believe that fluctuating asymmetry may be reflection of developmental instability, an organism's ability to buffer random accidents of development. Others believe that fluctuating asymmetry can be reduced to the level of randomness of thermal movement of particles. And there are those who believe that fluctuating asymmetry represents variation of exclusively environmental origin.

Directional asymmetry occurs when 'there is normally a greater development of a character on one side of the plane or planes of symmetry than on the other (Van Valen, 1962).' This type of asymmetry is consistent within a species. One example of directional asymmetry is the mammalian heart which is developmentally larger on the left side compared to the right. Palmer and Strobeck (1986, 1992) suggests that this type of asymmetry has a genetic basis.

Antisymmetry is a consistent asymmetry within a population, but it is unpredictable to which side of the organism will show greater development (Graham et *al.* 1993). It is presumed that antisymmetry has a genetic predisposition (Palmer and Strobeck, 1992). The most extreme forms of antisymmetry are characterized by a bimodal distribution of deviations from bilateral symmetry.

The causes of these types of asymmetry continue to be a controversy that is unresolved (Graham et *al.* 1993) and this particular research study will not focus on it.

Measuring Prevalence of Craniofacial Asymmetry

Interest and studies on human facial symmetry, or lack of, has been a subject of interest for over a century. Woo (1931) conducted direct chordal and arcual measurements on a large number of skulls from the 26th to the 30th Egyptian dynasties. He concluded that the human skull

is definitely and markedly asymmetric with cranial bones on the right side, on the whole, having more dominance over the left. The contralateral side of the facial complex exhibited an asymmetry with the left zygoma and left maxilla being larger. Vig and Hewitt (1975) looked at 63 posterior-anterior (PA) cephalometric radiographs to investigate facial asymmetry in terms of its components and demonstrated an overall facial asymmetry with the larger side being on the left. Similarly, Lundstrom (1961) measured 29 skulls and also found a tendency towards left side enlargement of the skull. Severt and Proffit (1997) reported prevalence of facial asymmetry to be between 21-85%. Varying prevalence of asymmetry has been reported in the different components of the face, upper face, midface, and chin, as well as with different sagittal occlusal problems (Severt & Proffit, 1997; Proffit & Turvey, 2003). Severt and Proffit's (1997) retrospective study using posterior-anterior (PA) cephalograms of orthognathic patients identified those with Class II skeletal patterns as being the least asymmetric, and that there was higher incidence of asymmetry in Class III, long face, and Class I patients. Other studies have also shown an increased incidence of mandibular asymmetry in patients with a Class III skeletal discrepancy (Reyneke *et al.,* 1997). Kilic *et al.* (2009), using PA radiographs, found that Class III skeletal groups tended to have greater skeletal asymmetries in the lower face. Kim *et al* (2011) examined and compared maxillofacial characteristics affecting chin deviation in facially asymmetric patients using 3D imaging; they found that subjects showed predominant left side deviation, regardless of mandibular retrusion or mandibular prognathism, with significantly different ramus lengths.

Other existing studies have evaluated the relationship of dental asymmetries, such as those seen in Class II subdivisions, and skeletal asymmetries. Sanders *et al.* (2010) concluded that the etiology of Class II subdivision malocclusions is primarily due to an asymmetric

mandible that is shorter and positioned more posteriorly on the Class II side. Kurt *et al* (2008) evaluated condylar and mandibular ramal asymmetry using panoramic films in patients with Class II subdivision malocclusions as well and found that these patients have symmetrical condyles, but discrepant condylar and ramal height measurements. One study compared Korean skeletal Class III patients with chin point deviations and found that compared to symmetric Class III patients, there was a significant difference in teeth positions, ramus height, and gonial position (Baek *et al.* 2007). Clinical situations demonstrating asymmetries results from an unequal growth of the dentofacial components; however, some situations may be exacerbated by a compensatory mechanism, such as a lateral functional dental shift due to a narrow maxilla or anterior dental relationship causing an anterior shift of the mandible (Cheny, 1961). Some asymmetries are only dental in nature and can result from habits relating to finger sucking habits, asymmetric chewing habits, loss of dental structure and contact points due to dental caries, early loss or extraction of primary or permanent teeth, or trauma. The ability to understand the exact size, shape, and position of underlying asymmetry is necessary to properly diagnose and treat patients who have asymmetries.

These findings support Fischer who, in 1954, stated that facial asymmetry is a natural phenomenon and there's nothing abnormal about it. He found that natural asymmetry of faces does not necessarily interfere with attainment of a correct dental occlusion, but the clinical significance of structural facial asymmetries lies in the fact that they are not amenable to change by only orthodontic means. Therefore, these asymmetries place certain limitations on orthodontic tooth movement and may require adjunctive orthognathic surgery to restore function and facial balance.

There are also studies that have focused on classifying and grouping the types of asymmetries seen in patients. Hwang *et al.,* (2007) looked at 2D radiographs and photographs of 100 consecutive orthodontic patients and found that there were five clusters based on three variables from frontal cephalograms: menton deviation, apical base midline discrepancy, and vertical difference between the right and left antegonion. Baek *et al.,* (2012) aimed to devise a systematic classification for diagnosis and surgical treatment of facial asymmetry. They evaluated 43 patients with apparent facial asymmetry and classified these patients into groups based on structural characteristics. They created four groups: 1) one group was based on mandibular body asymmetry; 2) another was related to condylar asymmetry leading to ramus height difference and menton deviation; 3) the third group involved maxillary canting and mandibular overriding (what is overriding); and 4) the last group was characterized by C-shaped asymmetry involving maxillary canting and deviation. Katsumata *et al.* (2005) created an asymmetry index using 3D-computed tomography imaging procedure for a 3-D coordinate point evaluation system to assess and diagnose patients with facial asymmetry. While these studies have furthered evaluated skeletal asymmetries, no single system has been implemented nor has a "gold standard" been accepted.

Three-Dimensional Imaging versus Two-Dimensional Imaging

The primary method for diagnosing maxillofacial deformities, including facial asymmetry, has been two-dimensional cephalometric radiography. Posteroanterior (PA) cephalograms, submentovertex projections, and lateral cephalograms have been widely used in orthodontic and orthognathic surgery planning for treatment of asymmetry. Although the PA cephalogram and submentovertex projections do offer valuable mediolateral information for

asymmetry and transverse evaluation of the dentoalveolar, and lateral cephalograms allow for a sagittal view of the craniofacial skeleton, these two-dimensional views also have limitations.

Two-dimensional cephalograms are a projection of a three-dimensional object onto a two-dimensional surface and is, therefore, subject to distortion and projection error. The images can be distorted by the patient's head position during the image process. Furthermore, evaluation and measurements made on the films are more difficult due to superimposition of cranial structures. Results in differences between actual linear measurements and measurements derived from PA cephalograms have been well documented (Trpkova *et al.* 2003). Due to superimposing images in a lateral cephalogram, it is difficult to determine the difference between the left and right side structures, and there is an issue with different enlargement ratios. (Bishara et al, 1998; Damstra *et al.,* 2011; Maeda *et al.,* 2006; Park *et al.,* 2006; Pirttiniemi *et al.,* 1996; Trpkova *et al.*, 2003; Baek *et al.,* 2012) Another disadvantage is that cephalometric landmarks are often widely separated and do not provide adequate information about spaces, curves, or spaces far from the midline (Terajima *et al.,* 2009). Panoramic radiographs have also been used to evaluate asymmetry, but lengths and angles cannot be measured accurately on the panoramic view (Terajima *et al.*, 2009).

The development of cone beam computed tomography (CBCT) has greatly reduces the issues associated with 2-D cephalograms. CBCT images are inherently more accurate due to the fact that the beam projection is orthogonal. This means that the x-ray beams are approximately parallel to one another and the object is very near the sensor. Therefore, there is very little projection effect. In addition, this effect is further corrected by the computer software, resulting in undistorted 1-to-1 measurements. This is in contrast to traditional imaging where there is always some projection error because the anatomic region of interest is some distance away from

the film (Lagravere *et al*. 2008). Additionally, the spatial image of the craniofacial structures can be produced and be rotated for ease of viewing (Park 2006). A benefit of CBCT landmark identification is a lack of superimposed structures, which creates easier visualization of certain skull regions. Previous research has also confirmed that landmark placement on three-dimensional systems were stable and effectively reproducible (Shibata *et al.* 2012).

At present, there are an increasing number of studies utilizing CBCT to attempt to identify and isolate skeletal asymmetries, but there is still a need for studies that can properly localize and quantify asymmetries in individuals. The presence of such asymmetries can sometimes be difficult to localize due to multiple asymmetric areas and compensation (Yanez-Vico *et al.,* 2010). A study by Hwang *et al.* (2012) confirmed that there were differences in bilateral craniofacial landmarks in the transverse, sagittal, and vertical planes; therefore, concluding that 3D evaluation would be essential to evaluate facial structures. Asymmetry of the dentofacial complex may be unilateral or bilateral, and can occur in the following directions: antero-posterior, supero-inferior, and medio-lateral.   As proper diagnosis of dentofacial asymmetries takes place in all three planes, two-dimensional cephalograms provides limited information and using three-dimensional imaging could prove clinically useful.

Geometric Morphometrics to Study Asymmetry

Orthodontists and biological anthropologists have common interests.   Just as in orthodontics, the field of biological anthropology studies shape and form, and has long recorded metric observations in an attempt to understand the way in which biological forms varied from one another, to establish the correspondence between form and function, and to quantify the description of characteristic traits. Orthodontists have been recording landmark data on two-

dimensional cephalometric radiographs to characterize skeletal jaw relationships. The desire to analyze biological forms in ways that preserve the physical integrity of form in two- or three-dimensions in biological anthropology led to the development of the statistical field of geometric mophometrics, defined as the fusion of geometry and biology (Bookstein, 1982). Geometric morphometrics avoids collapsing the form into series of linear or angular measures that do not include information pertaining to geometric relationships of the whole. In traditional orthodontic analyses and methods, capturing geometry by way of landmark data has become the standard. The use of landmarks has become widespread because landmarks are repeatable. They provide geometric information in terms of relative location of points, but salient features of morphology are overlooked when landmark data are used exclusively, and landmarks do not contain information on the spaces, curves, or spaces between them (Richtsmeier *et al.,* 2002). By borrowing the tools from the biological anthropology world, orthodontists can progress in their methods of understanding craniofacial structures to improve their diagnoses and classification systems.

In order to begin understanding geometric morphometrics, a few questions and definitions must first be provided.

What is shape?

Shape is all the geometric information that remains when location, scale, and rotational effects are filtered out from an object: it is invariant to Euclidean similarity transformations (Dryden and Mardia, 1998). This is different from "form" which is sometimes used to distinguish a set of landmarks that have a scale.

How does one describe shape?

One way to describe a shape is by locating a finite number of points on the outline. A <u>landmark</u> is defined as a point of correspondence on each object that matches between and within populations. Landmarks can be discriminated into three subgroups:

(1) <u>Anatomic landmarks</u> are points assigned by an expert that corresponds between organisms in some biologically meaningful way.

(2) <u>Mathematical landmarks</u> are points located on an object according to some mathematical or geometrical property, *i.e.,* high curvature or an extreme point.

(3) <u>Pseudo-landmarks</u> are constructed points on an object either on the outline or between landmarks.

To obtain a true shape representation, location, scale, and rotational effects need to be filtered and removed. This is obtained by establishing a coordinate reference to which all shapes are aligned. In this study, a Procrustes Analysis (*i.e.,* Procrustes superimposition, Procrustes fitting, generalized Procrustes analysis, generalized least squares, and least squares fitting) centers the centroid (defined as the center point of a shape, a sample of shapes, or a single landmark in a sample of shapes) of the object's landmark at an origin (0, 0, 0) and rotates each shape around the origin until the sum of squared distances among them is minimized. In geometric morphometrics, the main measure of difference is the Procrustes distance, the distance between two shapes after they have been superimposed.

Objective of Study

The objective of this study is to determine if there is a difference in type and quantity of asymmetry, in all three dimensions, between Class I, Class II, and Class III sagittal skeletal types using geometric morphometrics. The null hypothesis is that there is no difference in asymmetry

between skeletal Class I, II, and III patients. The hypothesis tested is that the presence and severity of craniofacial skeletal asymmetry is greater in patients that have a sagittal jaw relationship beyond one standard deviation of normal.

MATERIALS & METHOD

Subjects

The study's subjects were obtained using a convenience sample from a database of pre-treatment CBCT scans at the Division of Orthodontics, University of California at San Francisco. 440 subjects' were selected and anonymized. Subjects for this particular study were then identified using specific inclusion criteria. Inclusion criteria for subjects were as follows: females $\geq$ 14 years of age, males $\geq$ 16 years of age, subjects must have had a beginning record consisting of a 12" CBCT scan with reformatted lateral cephalometric radiograph to obtain ANB values, no prior orthodontic treatment, and no craniofacial anomalies or syndromes.

There were a total of 144 subjects: 62 were Class I (0 ° $\leq$ANB$\leq$4 °), 63 were Class II (ANB$\geq$4º), and 19 were Class III (ANB$\leq$0º). Tables 1 and 2 summarize characteristics of the sample.

Group (class)	n	# Male (Ave. age in years)	# Female (ave. age in years)	Ave. SNA(º)	Ave. SNB(º)	Ave. ANB (º)	Ave. MP-SN (º)
I	62	22	40	82.3	80.1	2.2	34.8
II	63	10	53	82.4	76.7	6.1	39.5
III	19	9	10	80.2	83.1	-2.8	33.2
	Total 144	41 (27.6)	103 (24.5)	81.6	80.0	1.8	35.8

Table 1. Summary of subjects.

Class II	13 protrusive maxilla, retrognathic mandible	30 retrognathic mandible, normal maxilla	20 protrusive maxilla, normal mandible
Class III	12 prognathic mandible, normal maxilla	7 retrusive maxilla, normal mandible	

Table 2. Further breakdown of Class II and Class III groups to identify primary jaw contributing to skeletal discrepancy.

This study was approved by the UCSF Institutional Review Board, the Committee on Human Research (#1000564), which included minors. Informed consent to participate in this study was obtained from each subject or, in the case of minors, guardian.

CBCT Imaging

Each subject had a full 12" CBCT scans were taken as part of the patient's beginning records on a Hitachi MercuRay (Hitachi Medico Technology, Tokyo, Japan) cone beam machine. The CBCT scans are stored as digital imaging and communications in medicine (DICOM) files. Amira software (Amira 3.1, Mercury Computer Systems GmbH, Berlin, Germany) was used to visualize the volumetric data of each subject and obtain appropriate thresholds to visualize the structures of interest. For our purposes, three thresholds were required to fully visualize the structures of the upper craniofacial structures, the condyles, and the mandible as all of these structures could not be visualized at one particular threshold without extra noise that would hinder the ability to landmark. The files were then converted and saved into a polygon file format (PLY) that defines a surface model.

Landmarking

Landmark placement was completed using Landmark Editor, a software developed by scientists at the Institute for Data Analysis and Visualization (IDAV) at the University of

California, Davis, and originally developed, for the purposes of analyzing, interpreting, and visualizing three-dimensional shapes of fossils under the statistical framework of geometric morphometrics. This landmark software allows landmarks to be easily placed on complex geometric surfaces. The software also allows one surface (in our case, the surface is the craniofacial structure) to be the "atlas," to which all others will be corresponded (homologue) in order to iteratively load other surfaces and semi-automatically apply all landmark information from the atlas surface onto the new surface. The semi-automatic application of landmarks can then be adjusted for each unique surface. The reason for the atlas surface is to coordinate the landmark primitives and to significantly reduce human error which is a problem that can occur when placing landmarks on several hundred surfaces (Landmark User Guide 3.6, 2007).

This study used 183 landmarks with 11 landmarks for midline structures. The other 172 landmarks were bilateral points and, therefore, paired (86 pairs) landmarks (Table 3, Figures 1-3).

Table 3. Description of landmarks.

	Landmark number	Midline or Bilateral	Type of landmark	Description
Landmarks 1-68: Refer to Fig. 1	1.	Midline	Anatomic	Glabella on frontal bone
	2.	Midline	Pseudo	Point midway between Point 1 and Point 3
	3.	Midline	Anatomic	Midline of Nasion
	4.	Midline	Pseudo	Midpoint of frontal spine of nasal bone
	5.	Midline	Anatomic	Anterior most point of anterior nasal spine
	6.	Midline	Pseudo	Midpoint on Intermaxillary suture between point 5 and 7
	7.	Midline	Anatomic	Point of transition from crown of most incisor crown to alveolar projection between maxillary central incisors
	8.	Bilateral	Anatomic	Medial border of fronto-zygomatic suture; on orbital rim
	9.	Bilateral	Anatomic	Superior most point of infraorbital foramen
	10.	Bilateral	Pseudo	Midway on frontal ridge between points #10 and 12

11.	Bilateral	Anatomical	Lateral border of fronto-zygomatic suture
12.	Bilateral	Pseudo	Lateral border of frontal process of zygomatic bone
13.	Bilateral	Mathematic	Most prominent point on lateral border of frontal process of zygomatic bone
14.	Bilateral	Pseudo	Lateral Border of frontal process of zygomatic bone, midway between points #14 and 16
15.	Bilateral	Mathematic	Where frontal process intersects with temporal process of zygomatic bone
16.	Bilateral	Pseudo	Superior border of zygomatic arch that divides distance between points #16 and #19 into equal thirds
17.	Bilateral	Pseudo	Superior border of zygomatic arch that divides distance between points #16 and #19 into equal thirds
18.	Bilateral	Mathematic	Where zygomatic arch meets flat surface of temporal bone
19.	Bilateral	Anatomic	Inferior most point of post-glenoid process
20.	Bilateral	Anatomic	Superior most point of glenoid fossa
21.	Bilateral	Mathematic	Inferior most point of articular eminence
22.	Bilateral	Pseudo	Inferior border of zygomatic arch
23.	Bilateral	Pseudo	Inferior border of zygomatic arch
24.	Bilateral	Pseudo	Inferior border of zygomatic arch
25.	Bilateral	Pseudo	Inferior-lateral border of zygomatic bone
26.	Bilateral	Pseudo	Approximately where zygomatic bone articulates with maxillary bone
27.	Bilateral	Pseudo	Lateral border of maxillary bone
28.	Bilateral	Pseudo	Lateral border of maxillary bone
29.	Bilateral	Mathematic	Alveolar process of approximate location of maxillary second molar
30.	Bilateral	Mathematic	Alveolar process, approximate location of maxillary first molar
31.	Bilateral	Mathematic	Alveolar process, approximate location between maxillary bicuspids
32.	Bilateral	Mathematic	Alveolar process, approximate location of maxillary canine
33.	Bilateral	Mathematic	Alveolar process, approximate location of maxillary lateral incisor
34.	Bilateral	Pseudo	Supraorbital margin
35.	Bilateral	Pseudo	Supraorbital margin
36.	Bilateral	Pseudo	Supraorbital margin
37.	Bilateral	Pseudo	Medial orbital rim
38.	Bilateral	Pseudo	Medial orbital rim

39.	Bilateral	Pseudo	Medial orbital rim
40.	Bilateral	Pseudo	Medial orbital rim
41.	Bilateral	Pseudo	Infraorbital rim
42.	Bilateral	Pseudo	Orbitale – lowest spoint on inferior margin of orbit
43.	Bilateral	Pseudo	Infraorbital rim
44.	Bilateral	Pseudo	Lateral orbital rim
45.	Bilateral	Pseudo	Lateral orbital rim
46.	Bilateral	Mathematical	Frontal process of maxillary bone, lateral rim of nasal cavity that converges with nasal bone
47.	Bilateral	Pseudo	Lateral rim of nasal cavity, point that divides approximate height of nasal cavity into quarters
48.	Bilateral	Pseudo	Lateral rim of nasal cavity, approximately mid-height of nasal cavity
49.	Bilateral	Pseudo	Lateral rim of nasal cavity, one quarter of height of nasal cavity
50.	Bilateral	Mathematic	Inferior lateral corner of nasal cavity
51.	Bilateral	Pseudo	Midpoint between point #53 and anterior nasal spine
52.	Bilateral	Pseudo	On flat surface of zygomatic arch, approximately at mid height of arch
53.	Bilateral	Pseudo	On flat surface of zygomatic bone where temporal process meets maxillary process, mid height of bone
54.	Bilateral	Pseudo	Most prominent point on maxillary process of zygomatic bone (may be at intersection of zygomatic and maxillary bone)
55.	Bilateral	Pseudo	Maxillary bone
56.	Bilateral	Pseudo	Between medial orbital rim and lateral rim of nasal cavity, on frontal process of maxillary bone
57.	Bilateral	Pseudo	Alveolar process of maxillary bone
58.	Bilateral	Pseudo	Alveolar process of maxillary bone
59.	Bilateral	Pseudo	Frontal process of zygomatic bone
60.	Bilateral	Pseudo	Frontal process of zygomatic bone
61.	Bilateral	Pseudo	Frontal bone
62.	Bilateral	Pseudo	Frontal bone
63.	Bilateral	Pseudo	Frontal bone
64.	Bilateral	Pseudo	Frontal bone
65.	Bilateral	Pseudo	Frontal bone
66.	Bilateral	Pseudo	Frontal bone
67.	Bilateral	Mathematic	Lateral suture of nasal bone at junction

				with frontal bone
	68.	Bilateral	Mathematic	Intersection of nasal bone with frontal bone
Landmarks 69-88: Refer to Fig. 2	69.	Midline	Anatomic	Infradentale (point of transition from crown of mandibular central incisors to alveolar projection)
	70.	Midline	Mathematical	Point B/ supramentale (deepest midline point on the mandible between infradentale and pogonion
	71.	Midline	Mathematical	Pogonion (most prominent point on chin)
	72.	Midline	Anatomic	Menton
	73.	Bilateral	Anatomic	Corresponds to approximate dental alveolar location of mid-buccal of mandibular second molar
	74.	Bilateral	Anatomic	Corresponds to approximate dental alveolar location of mid-buccal of mandibular first molar
	75.	Bilateral	Anatomic	Corresponds to approximate dental alveolar location of mid-buccal of mandibular second premolar
	76.	Bilateral	Anatomic	Corresponds to approximate dental alveolar location of mid-buccal of mandibular first premolar
	77.	Bilateral	Anatomic	Corresponds to approximate dental alveolar location of mid-buccal of mandibular canine
	78.	Bilateral	Anatomic	Corresponds to approximate dental alveolar location of mid-buccal of mandibular lateral incisor
	79.	Bilateral	Anatomic	Superior border of mental foramen
	80.	Bilateral	Mathematic	Lateral, most inferior border of mandibular symphysis
	81.	Bilateral	Pseudo	
	82.	Bilateral	Anatomic	Antegonial notch (most superior portion of the concavity present on lower edge of mandible)
	83.	Bilateral	Anatomic	Gonion (lower portion of the gonial angle)
	84.	Bilateral	Pseudo	Superior posterior point of gonial angle
	85.	Bilateral	Pseudo	Mid-height of posterior border fo ramus
	86.	Bilateral	Pseudo	Mid-width and mid-height of ramus
	87.	Bilateral	Pseudo	Mid-height of anterior border of ramus
	88.	Bilateral	Mathematic	Superior point of oblique line
Lan dm	89.	Bilateral	Anatomic	Most lateral point of condyle
	90.	Bilateral	Anatomic	Most medial point of condyle
	91.	Bilateral	Pseudo	Mid-width of anterior condylar head

|	92.	Bilateral	Pseudo	Posterior border at transition point from head to neck of condyle
	93.	Bilateral	Pseudo	Posterior transition point of concavity of coronoid notch
	94.	Bilateral	Mathematic	Lower point of depression or coronoid notch
	95.	Bilateral	Pseudo	Anterior transition point of concavity of coronoid notch
	96.	Bilateral	Anatomic	Most superior point of coronoid process
	97.	Bilateral	Pseudo	Anterior border of coronoid process, at height of coronoid notch
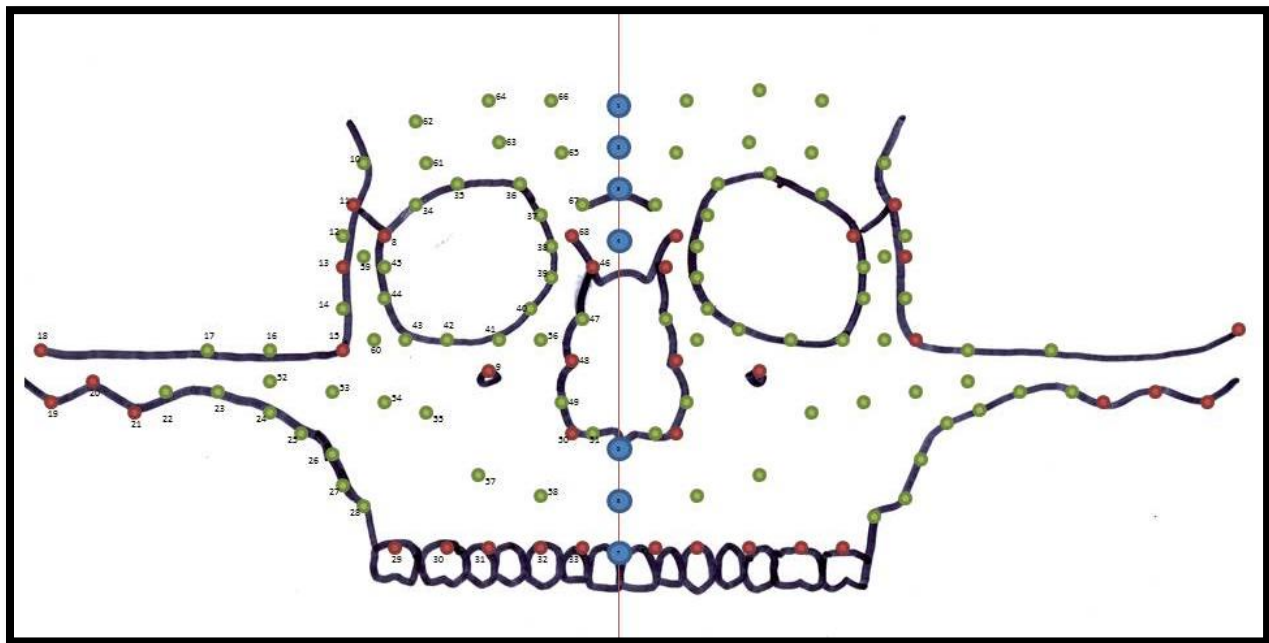
Figure 1. Landmarks 1-68.
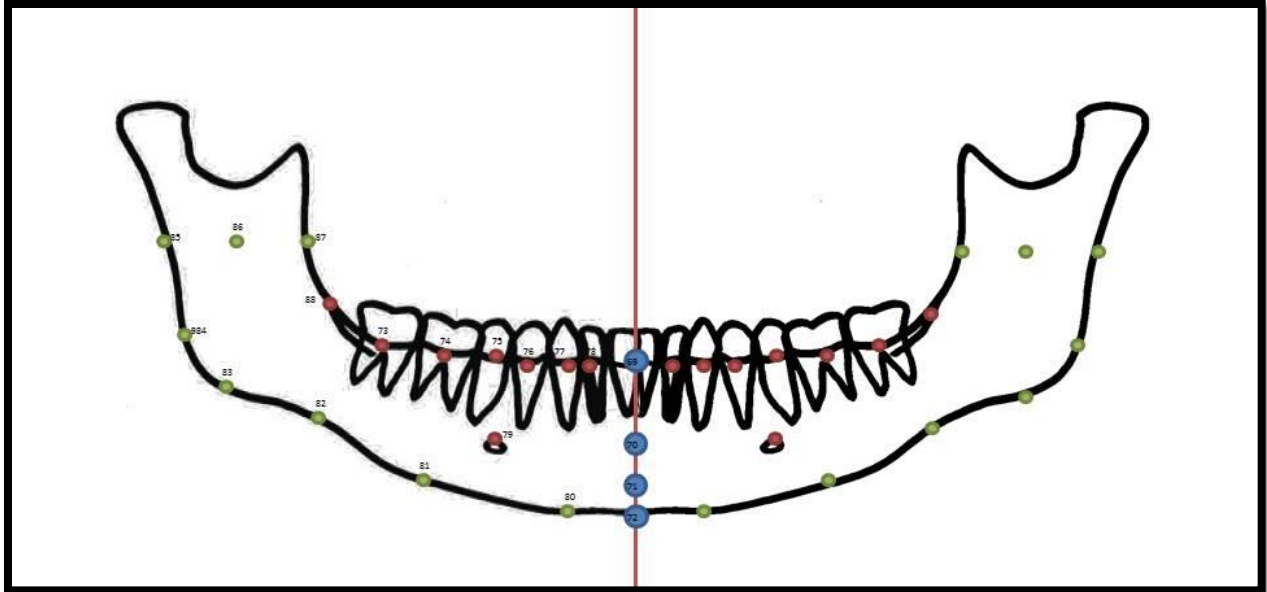
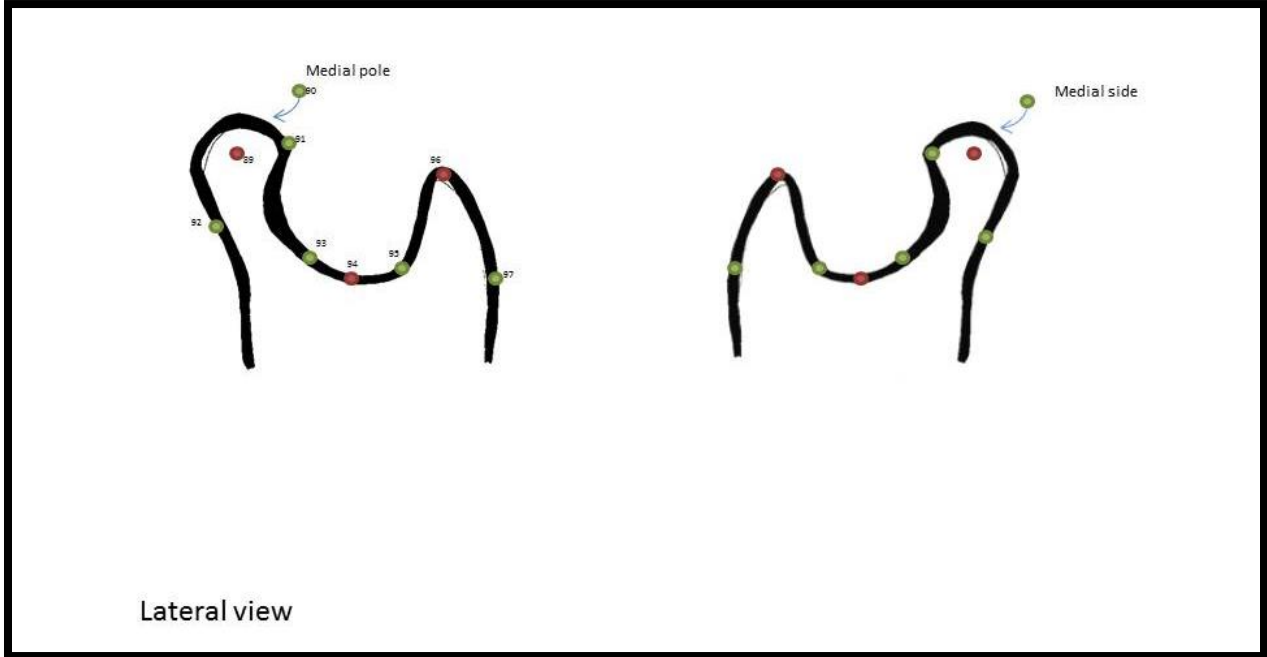**Figure 2.** Landmarks 69-88.

Figure 3. Landmarks 89-97.

Statistical Analysis

To obtain a true shape representation, location, scale, and rotational effects need to be filtered out. Therefore, a Procrustes analysis, also known as a Procrustes

17

superimposition, is utilized to obtain such a coordinate reference (Bookstein, 1991; Dryden and Mardia, 1998). Generalized Procrustes superimposition superimposes specimen landmark configurations by translating them to a common origin, scaling them to unit centroid size (the square root of the sum of squared distances of all landmarks to the centroid of the object), and rotating them according to a best-fit criterion. This ensures that the differences in shapes are minimized.   Permutation test was performed on the Procrustes distance between the group mean configurations. In other words, given a distance between the means of two groups, it calculates the probability that both groups derive from the same mean (i.e., that the calculated difference is not significant).

Principal Component Analysis (PCA) is a data reduction procedure and employed as a means to identify patterns in a set of data. It expresses the data in such a way as to highlight their similarities and differences. PCA finds the axes of greatest variation in a data set and develops and summarizes the total variance in a data set by rotating it so that the principal components explain progressively smaller amounts of the total variance. Extracted principal component scores are used for other statistical analyses including Hartigan's dip test. The dip test measures the departure of a sample from unimodality (Hartigan and Hartigan, 1985).

All the geometric morphometric procedures and statistical analyses were carried out with MORPHOJ software package (Klingenberg, 2011).

RESULTS

Generalized Procrustes Superimposition was completed for 183 landmarks for the 144 subjects (Figure 4). Permutation tests (10,000 permutation rounds) for the asymmetric

component were conducted and indicated that there is a significant difference of Procrustes

distances between the Class I and Class III groups (*p*=0.0006), and Class II and Class III groups

(*p*=0.0003) (Table 4). There was no significant difference between the Class I and Class II group

(*p*=0.6742).

Table 4. Procrustes distances of each group (*p-value from permutation tests*).
indicates statistical significance

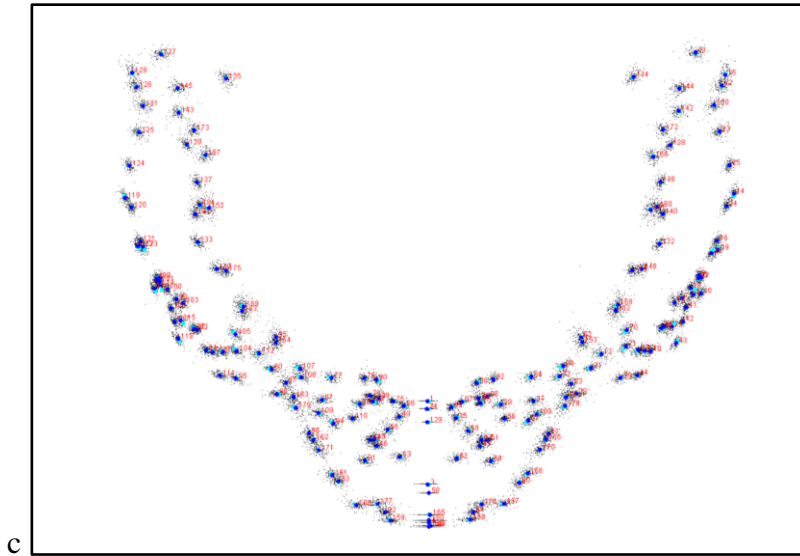|	Class I	Class II
Class II	0.0039 (*0.6742*)	
Class III	0.0099 (*0.0006**)	0.0095 (*0.0003*)

c
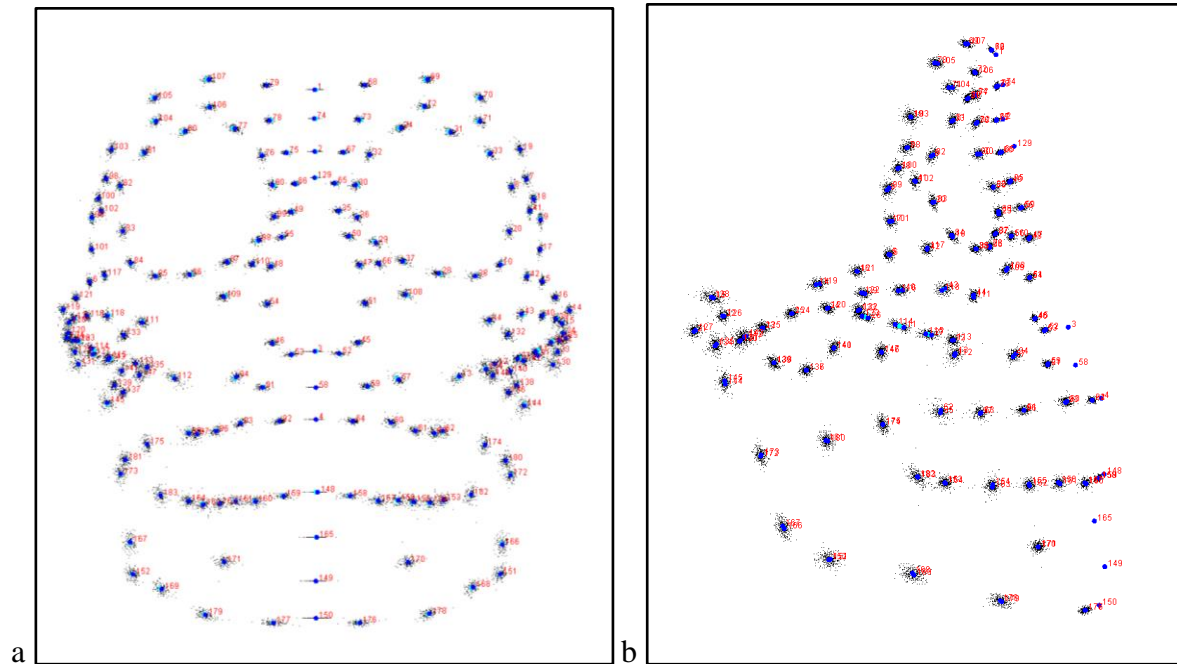
Figure 4. Generalized Procrustes Superimposition for all landmarks and all subjects. (a) Frontal view; (b) Sagittal view; (c) Superior-inferior view.

A total of 143 principal components were identified (Figure 5). The first, and largest, principal component accounts for 13.485% of the total variance observed in the subject population. The other principal components will not be discussed as the next largest principal component (PC2) accounts for almost less than half of the first component (Table 5).

The average skeletal Class I, Class II, and Class III PC1 scores were -0.00129, -0.00065, and 0.00637 (Table 6). The difference between these scores were statistically significant ($p>0.05$) for Class I versus Class III, as well as Class II versus Class III; there was no significant difference between Class I and Class II groups (Figure 6). The variance for the Class I, Class II, and Class III groups were 0.0000764, 0.0000549, and 0.0000939 respectively. The differences in variances were not statistically significant. Although the difference in variance is not statistically significant, it should be noted that the Class III group does display the largest variance. This could possibly lie in the fact that asymmetries tend to be fluctuating and could deviate to the right or left.

20

Visualization of principal component 1 reveals that the greatest magnitude of asymmetry lies in the anterior mandible with deviation towards the left with variable compensations in the remaining craniofacial structure (Figure 7).

Distributions of PC scores were also evaluated via density curves and Hartigan's Dip Test, focusing exclusively on the mandibular landmarks as the major asymmetries were localized in this region (Figure 8). The Class I and Class II groups yielded a dip statistic (D) of 0.0356 (p=0.8502) and 0.027 (p=0.9914), both of which were not statistically significant, indicating a unimodal distribution. The Class III group produced a dip statistic of 0.1058 (p=0.0599), which, even at a small sample (n=19), approaches statistical significance and suggests a bimodal distribution.
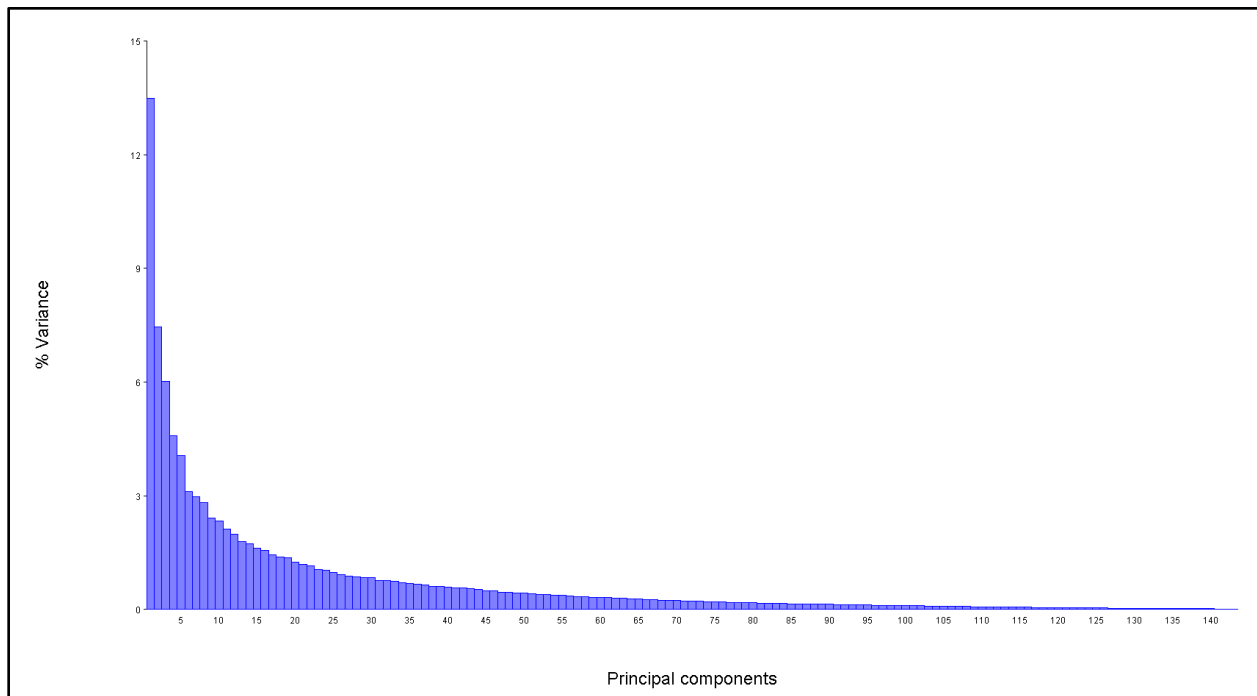

Figure 5. Scree plot of principal components and their associated percentage variance.

Table 5. Percentage Variance of first ten of 143 principal components.

Principal Component	Eigenvalues	% Variance	Cumulative %
1	**0.00007454**	**13.485**	**13.485**
2	0.00004123	7.460	20.945
3	0.00003327	6.018	26.963
4	0.00002532	4.580	31.543
5	0.00002242	4.056	35.599
6	0.00001716	3.105	38.704
7	0.00001639	2.966	41.670
8	0.00001555	2.813	44.483
9	0.00001329	2.404	46.886
10	0.00001288	2.331	49.217

Table 6. Average PC1 scores and variance for each skeletal group.

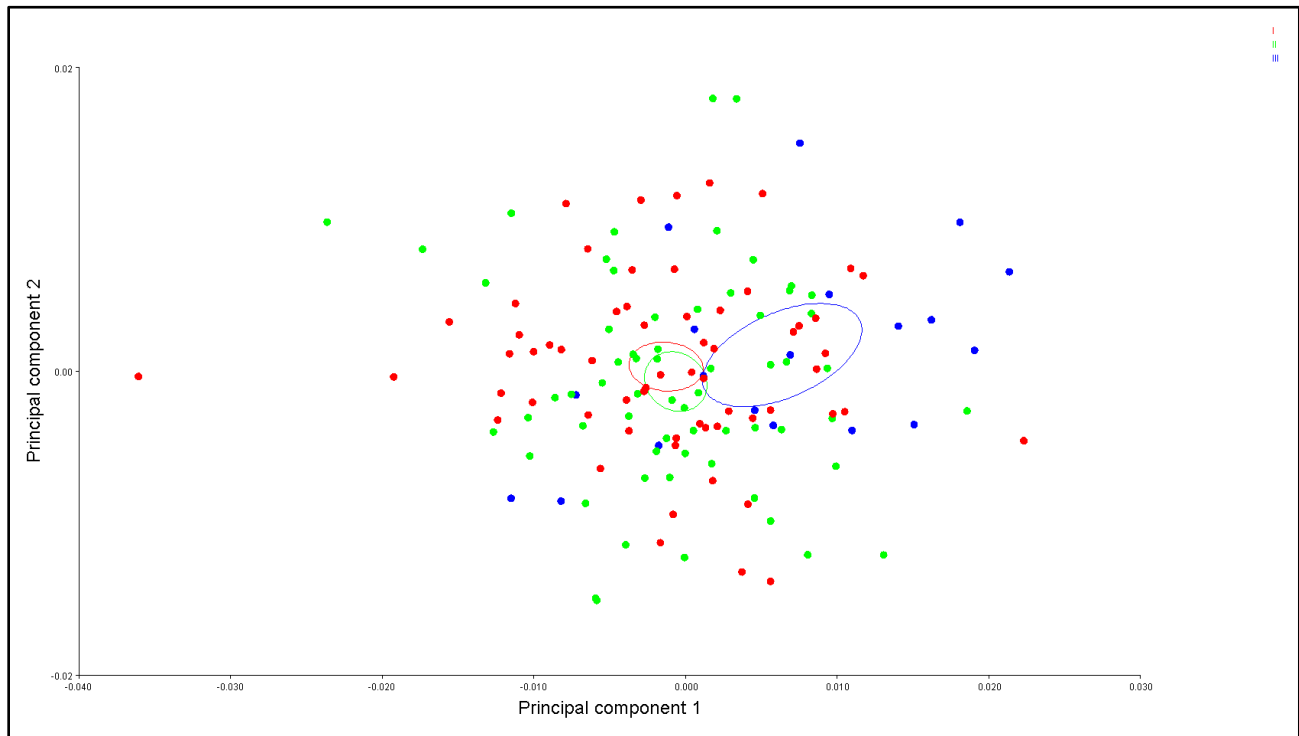|	Average PC1 Score	Variance
Class I	-0.0012908	0.0000764
Class II	-0.0006501	0.0000549
Class III	0.0063678	0.0000939

Figure 6. Principal component 1 versus principal component 2 with all 183 subjects. Subjects are colored by their skeletal class with corresponding 90% confidence ellipse: Class I group (red), Class II group (green), and Class III group (blue).
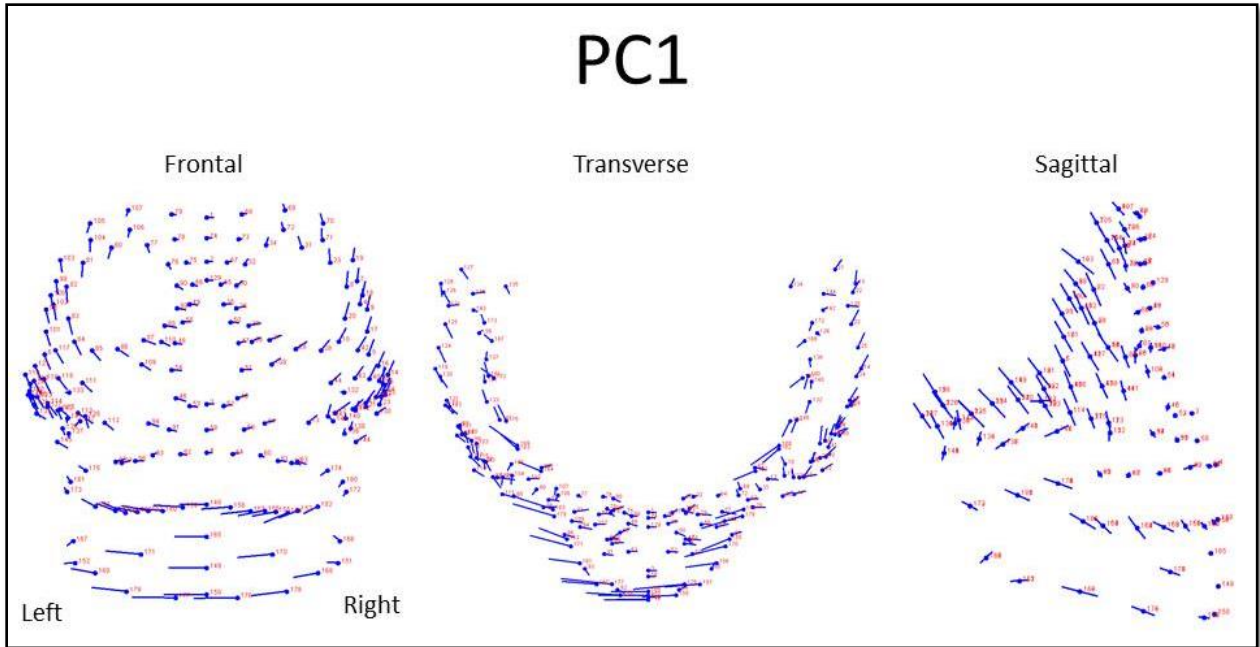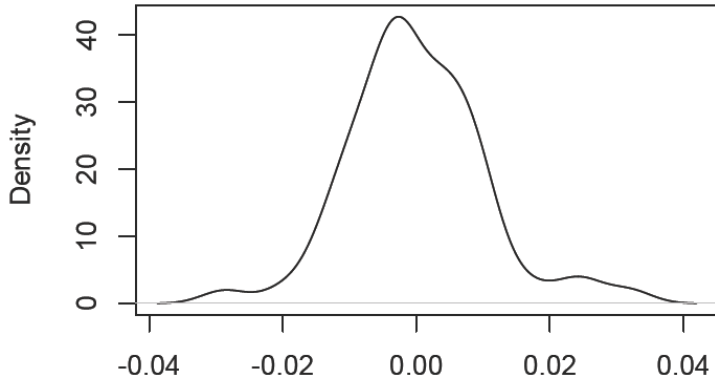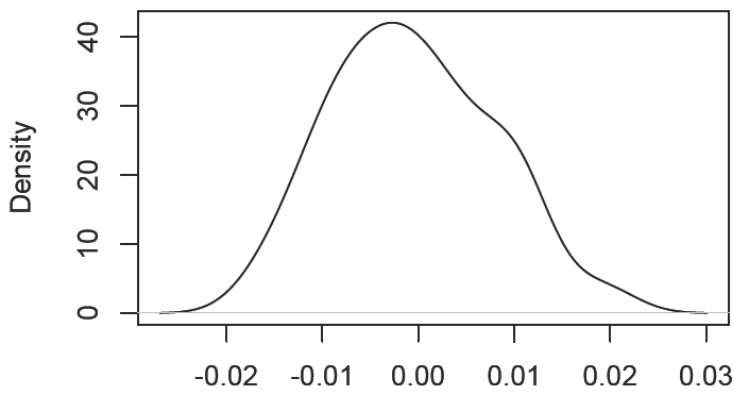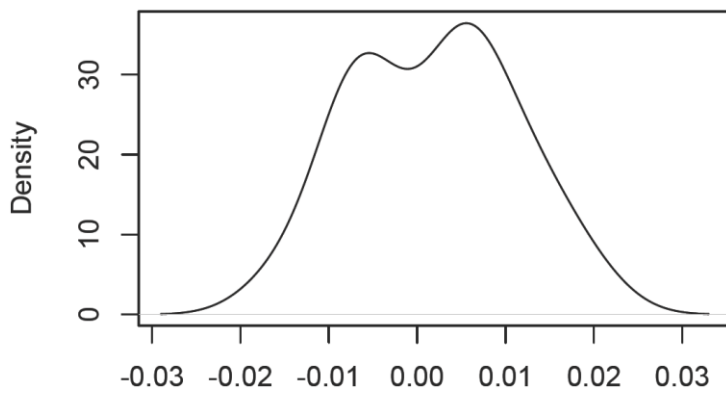
Figure 7. Principal component 1.

A

B

C

Figure 8. Density curves of mandibular landmarks for (A) Class I, (B) Class II, and (C) Class III groups.

The Class III sample was further assessed independent of the other groups. Of the 19 Class III subjects included in the study, 12 were diagnosed with a prognathic mandible and seven had a retrusive maxilla as the primary problem jaw contributing to their skeletal malocclusion. A PCA was performed to see if there was a difference in asymmetry related to the problematic jaw. Eighteen PCs were identified with PC1 contributing 20.91% of the total variance observed (Figure 9, Table 7). Visually, PC1 for the Class III group was similar to PC1 for all groups combined with the greatest magnitude of asymmetry in the anterior mandible towards the left (Figure 10).

When comparing the subset of Class III patients who had a normal maxilla and prognathic mandible against the Class III patients with a retrusive maxilla and normal mandible, the difference between the mean PC1 scores and variance were not statistically significant ($p>0.05$) (Figure 11). The mean PC1 score for the prognathic mandible group was -0.00039 with a variance of 0.00012. The mean PC1 score for the retruded maxilla group was 0.00067 with a variance of 0.00016.
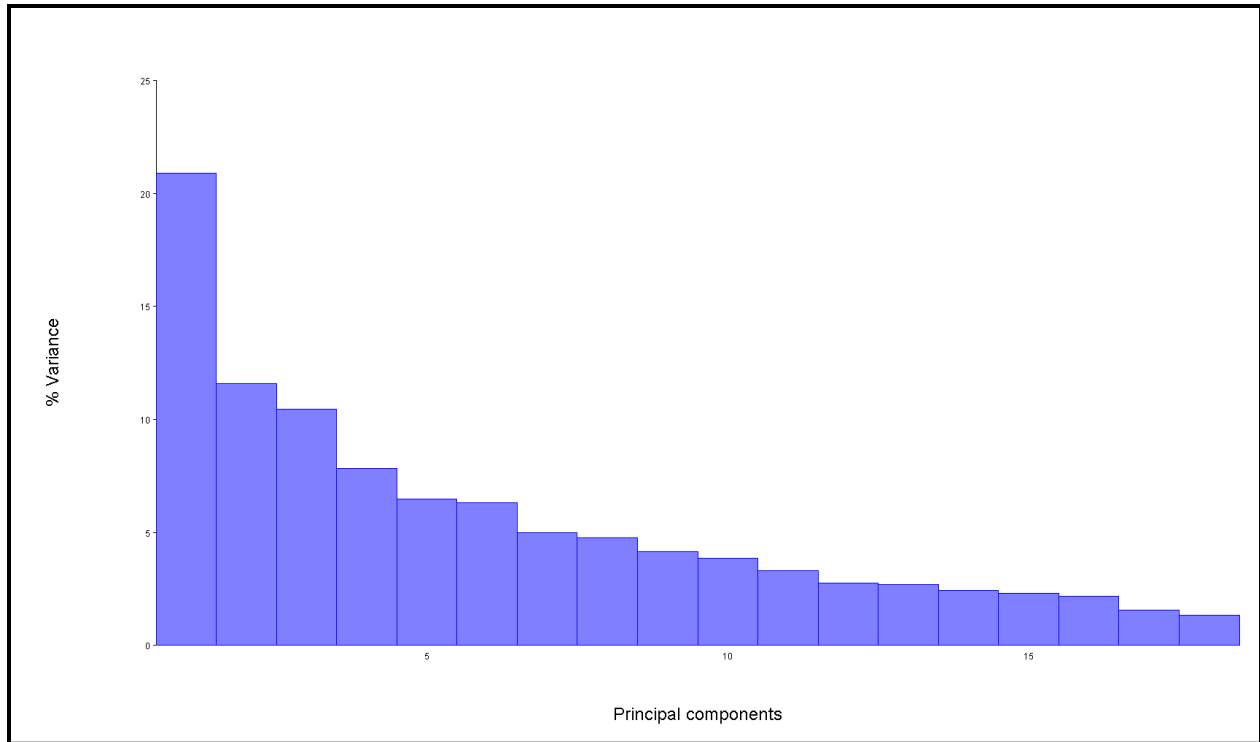
Figure 9. Scree plot of principal components and their associated percentage variance for the Class III sample.

Table 7. Percentage Variance of all principal components for the Class III sample.

| Principal Component	Eigenvalues	% Variance	Cumulative %
1	0.00012701	20.910	20.910
2	0.00007037	11.586	32.496
3	0.00006353	10.459	42.954
4	0.00004755	7.828	50.782
5	0.00003943	6.492	57.274
6	0.00003833	6.310	63.585
7	0.00003033	4.993	68.578
8	0.00002890	4.758	73.335
9	0.00002530	4.165	77.500
10	0.00002340	3.852	81.352
11	0.00002019	3.324	84.675
12	0.00001684	2.773	87.448
13	0.00001644	2.707	90.155
14	0.00001474	2.427	92.582
15	0.00001406	2.315	94.897
16	0.00001325	2.182	97.079
17	0.00000959	1.579	98.657
18	0.00000815	1.343	100.000

26
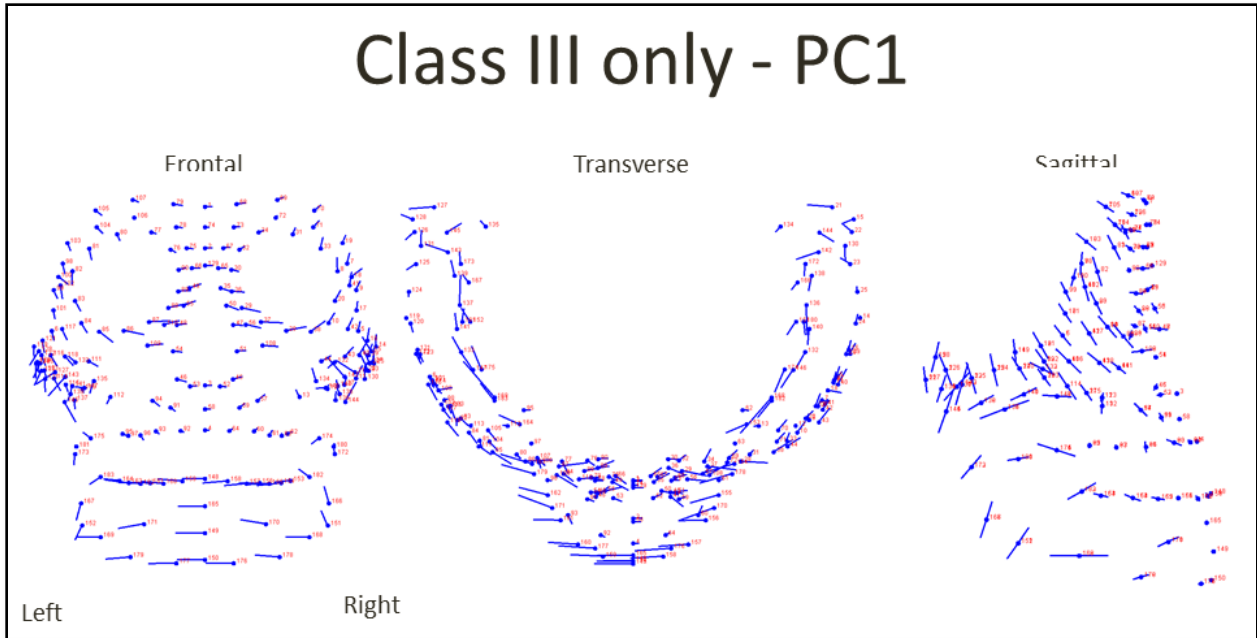
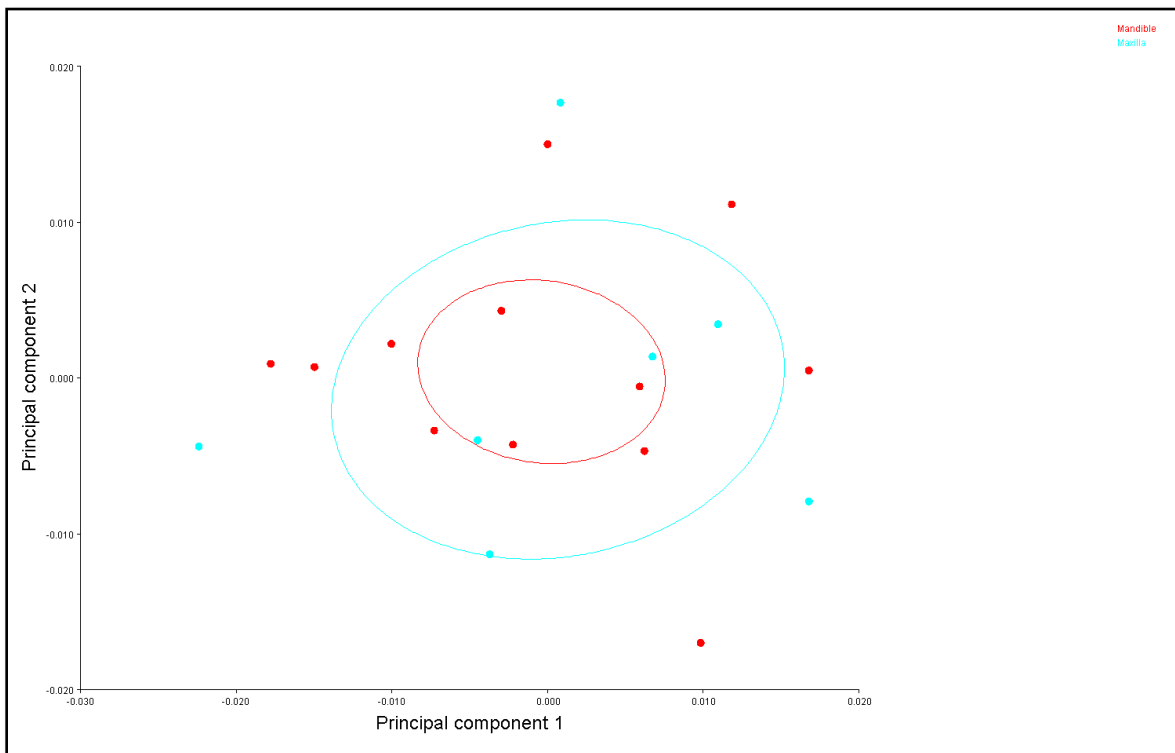**Figure 10.** Principal component 1 for the Class III sample.

Figure 11. Principal component 1 versus principal component 2; data set only includes the 19 Class III subjects. The red subjects are those with a prognathic mandible/normal maxilla (n=12); the teal subjects are those with a retrusive maxilla/normal mandible (n=7); 90% confidence ellipses are illustrated.

There were a total of 103 females and 41 males included in this study. Of the 103 females, 40 were Class I, 53 were Class II, 10 were Class III. Of the 41 males, 22 were Class I, 10 were Class II, 9 were Class III. The mean PC1 score for females was -0.00064 with a variance of 0.000082. The mean PC1 score for males was 0.00162 with a variance of 0.00005. An unpaired, two-tailed t-test showed that there was no significant difference ($p > 0.05$) between the mean PC1 scores or variance between males and females (Figure 12).
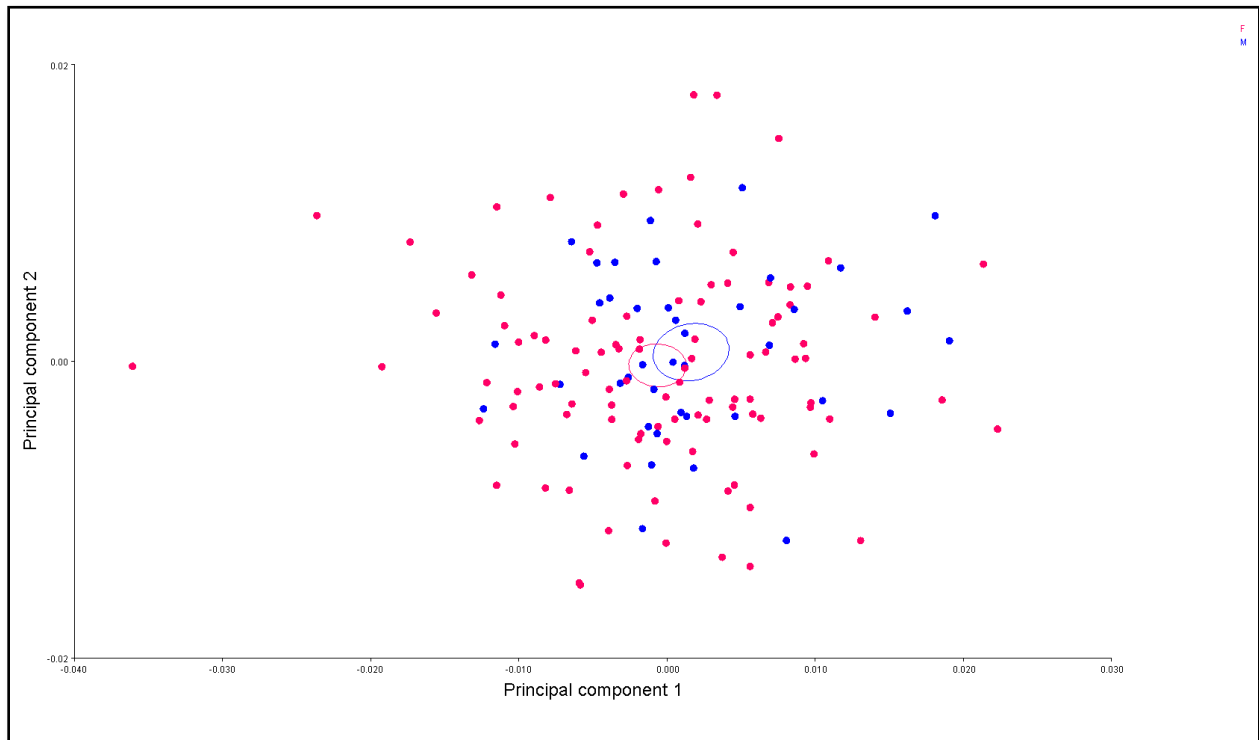

Figure 12. Principal component 1 versus principal component 2; Females are labeled in red and males are labeled in blue with their associated 90% confidence ellipse.

DISCUSSION

Orthodontic diagnosis and treatment planning has been and is still presently dominated by diagnosis based on piecing together information collected from a combination of two-dimensional lateral cephalograms, panoramic films, and posterior-anterior films. 3D CBCT imaging in the orthodontic field is transforming how clinicians can view and study their patients.

It allows the clinician to extrapolate a greater deal of information that is otherwise, unobtainable in all the combinations of 2D films. Asymmetry has traditionally been a discussion of bilateral discrepancies between the right and left parts. The introduction of 3D imaging into the discussion and study of asymmetry now allows us to evaluate asymmetries not only in terms of right-left, but also, inferior-superior, and anterior-posterior. Geometric morphometrics and 3D landmarking has allowed given us a method and tool to pinpoint localized regions of asymmetry and the accompanying compensations in the craniofacial skeleton between different subjects. In this study, when looking at the entire sample of subjects, the greatest variance of asymmetry was localized to the anterior mandible as visualized by the first principal component (Figure 7, Figure 10). The lengths and direction of each vector is significant for magnitude and direction of asymmetry.   It is apparent that as the anterior mandible goes towards the left, the rest of the craniofacial region compensates such that the left ramus and condyle appears to get shorter vertically while the right ramus and condyle regions lengthen vertically. Both sides of the mandibular body exhibit opposing anterior-posterior directions of compensation; sagitally, the left side shortens and the right side lengthens. In the upper craniofacial region, compensations are also apparent such that the left side shortens vertically with minor sagittal length decrease. The right counterpart of the upper craniofacial region lengthens vertically and slightly increases in the sagittal dimension. The finding that there is markedly greater asymmetry left of the facial midline supports Vig and Hewitt's 2D radiographic study that (1975) found that the face tended to deviate to the left in the lower third of the face in 67% of their subjects. Also, the results correspond to Kim et al.'s (2011) study that that used 3D imaging and found greater left side deviation as well, regardless of mandibular retrusion or mandibular prognathism, as well as significantly different ramus lengths. PCA and t-tests of just our Class III data confirmed that

there is no statistically significant difference in asymmetry between a skeletal Class III caused by

a retruded maxilla or prognathic mandible.

When the mean PC1 scores between females and males was compared, it was found that there

was no significant difference in asymmetry between genders.

The permutation test of the Procrustes distances of the subjects confirms that the skeletal

Class III patients were significantly different from that Class I and Class II patients such that

they are more likely to exhibit the asymmetries just discussed. This finding is in agreement with

Severt and Proffit's (1997) study that identified higher incidence of asymmetry in Class III

patients and less asymmetry in Class I patients; however, unlike our study's findings that Class I

patients did not find increased asymmetry, the Severt and Proffit (1997) study found Class I

patients exhibited more asymmetry. Our results also support Reyneke et al.'s (1997) findings

that showed an increased incidence of mandibular asymmetry in patients with a Class III skeletal

discrepancy.

The density graphs (Figure 8.a-c.)of the different skeletal Class groups' PC scores show

that the Class I and Class II groups have a normal, unimodal distribution centered around zero

(zero indicates symmetry). However, the Class III group shows a distribution with a dip statistic

that approaches significance (p=0.0599). This dip in the distribution is meaningful such that it

suggests there may be a bimodal distribution of asymmetries seen in skeletal Class III patients.

The higher peak indicates that there tends to be greater asymmetries towards the left, but the

other peak indicates a set of patients who also display asymmetries towards the right. A bimodal

distribution is representative of antisymmetry (Figure 13b). Antisymmetry presumably results

from a genetic predisposition, of unknown fraction, of individuals towards asymmetry, but

within a given sample, some individuals develop a left bias while others develop a right bias (Palmer and Strobeck, 1992).

In a population with fluctuating asymmetries, the right-left asymmetries seen are attributed to random effects and cancel each other out such that the frequency distribution has a parametric mean of zero and the variation is normally distributed about this mean (Palmer and Strobeck, 1992) (Figure 13a). The Class I and Class II groups exemplify such a distribution. This frequency distribution is commonly interpreted as a product of non-genetic variation in symmetry so the asymmetries seen in these populations may be attributed to developmental instability (Graham et al. 1993).
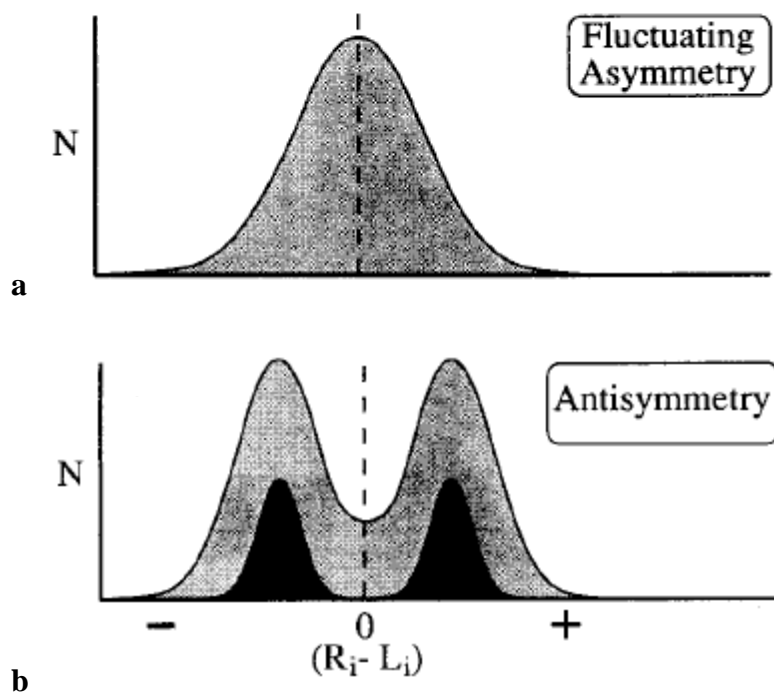

Figure 13. Example of a normal distribution representative of fluctuating asymmetry (a) and a bimodal distribution representative of antisymmetry (b).

CONCLUSIONS

- The amount of asymmetry detected in skeletal Class III subjects is statistically significant when compared to the skeletal Class I and Class II subjects. There was no difference in asymmetry between Class I and Class II subjects.

- The most significant asymmetry detected was localized to the anterior symphysis of the mandible which tended to deviate towards the left, regardless of mandibular prognathism or maxillary retrusion within the Class III subjects.

- While the greatest skeletal asymmetry was detected in the anterior mandible, there were also corresponding compensations in the mandibular ramus, condyles, maxillary, zygomatic, and orbital regions.

- The skeletal Class III group exhibit a bimodal distribution of asymmetry, indicative of antisymmetry, which suggests that there is a genetic predisposition for asymmetry.

- There was no difference in asymmetry between females and males.

REFERENCES

1. Baek C, Paeng JY, Lee JS, Hong J. *Morphologic evaluation and classification of facial asymmetry using 3-dimensionalcomputed tomography*. J Oral Maxillofac Surg. 2012 May;70(5):1161-9.

2. Baek SH, Cho IS, Chang YI, Kim MJ. *Skeletodental factors affecting chin point deviation in female patients with class III malocclusion and facial asymmetry: a three-dimensional analysis using computed tomography.* Oral Surg Oral Med Oral Pathol Oral Radiol Endod. 2007 Nov;104(5):628-39.

3. Bishara S, Burkey P, Kharouf J. *Dental and facial asymmetries: a review*. Angle Orthodontist 1994; 64: 89-98.

4. Bookstein F. *Foundations of Morphometrics*. Ann Rev Ecol Syst 1982; 13:451-470.

5. Bookstein, F. 1991. *Morphometric tools for landmark data: geometry and biology*. Cambridge University Press, Cambridge, 435 pp.

6. Cattaneo, P.M. and B. Melsen. *The use of cone-beam computed tomography in an orthodontic department in between research and daily clinic*. World J Orthod, 2008. 9(3): p. 269-82.

7. Cheney EA. *Dentofacial asymmetries and their clinical significance*. Amer J Orthod 1961;47:814-829.

8. Damstra J, Fourie Z, Ren Y. *Evaluation and comparison of postero-anterior cephalograms and cone-beam computed tomography images for the detection of mandibular asymmetry*. Eur J Orthod 2013; Feb;35(1):45-50.

9. Dryden, I. L. and Mardia, K. V. (1998) *Statistical Shape Analysis*. John Wiley, Chichester. 347 + xvii.

10. Fischer B. *Asymmetries of the dentofacial complex.* Angle Orthodontist 1954; 24: 179-192.

11. Graham J, Freeman D, Emlen J. *Antisymmetry, directional asymmetry, and dynamic morphogenesis.* Genetica 1993; 89:121-137.

12. Hartigan J, Hartigan P. *The Dip Test of Unimodality.* The Annals of Statistics 1985; 13(1): 70-84.

13. Hwang HS, Youn IS, Lee KH, Lim HJ. *Classification of facial asymmetry by cluster analysis.* Am J Orthod Dentofacial Orthop. 2007 Sep;132(3):279.e1-6.

14. Hwang HS, Yuan D, Jeong KH, Uhm GS, Cho JH, Yoon SJ. *Three-dimensional soft tissue analysis for the evaluation of facial asymmetry in normal occlusion individuals.* Korean J Orthod. 2012 Apr;42(2):56-63.

15. Katsumata A, Fujishita M, Maeda M, Ariji Y, Ariji E, Langlais RP. *3D-CT evaluation of facial asymmetry.* Oral Surg Oral Med Oral Pathol Oral Radiol Endod. 2005 Feb;99(2):212-20.

16. Kilic N, Kilic SC, Catal G. *Facial asymmetry in subjects with class III malocclusion.* Aust Orthod J. 2009 Nov;25(2):158-62.

17. Kim EJ, Palomo JM, Kim SS, Lim HJ, Lee KM, Hwang HS. *Maxillofacial characteristics affecting chin deviation between mandibular retrusion and prognathism patients.* Angle Orthod. 2011 Nov;81(6):988-93.

18. Klingenberg, C.P. (2011). MorphoJ: an integrated software package for geometric morphometrics. Mol. Ecol. Resour 11, 353–357.

19. Kurt G, Uysal T, Sisman Y, Ramoglu SI. *Mandibular asymmetry in Class II subdivision malocclusion.* Angle Orthod. 2008 Jan;78(1):32-7.

20. Lundstrom A. *Asymmetries of the dental arches, jaws, and skull, and their etiological significance.* Amer J Orthod 1961;47:26.

21. Maeda M, Katsumata A, Ariji Y, Muramatsu A, Yoshida K, Goto S, Kurita K, Ariji E. *3D-CT evaluation of facial asymmetry in patietns with maxillofacial deformities.* Oral Surg Oral Med Oral Pathol Oral Radiol Endod 2006; 102:382-390.

22. Palmer A, Strobeck C. *Fluctuating asymmetry: measurement, analysis, patterns.* Annual Review of Ecology and Systematics 1986; 17: 391-421.

23. Palmer A, Strobeck C. *Fluctuating asymmetry as a measure of developmental stability: implications of non-normal distributions and power of statistical tests.* Acta Zoologica Fennica 1992; 191: 57-72.

24. Park S, Yu H, Kim K, Lee K, Baik H. *A proposal for a new analysis of craniofacial morphology by 3-dimensional computed tomography.* Am J Orthod Dentofacial Orthopedics 2006; 129:600e.23-600.e34.

25. Pirttiniemi, P., Miettinen, J., and Kantomaa, T. *Combined effects of errors in frontal-view asymmetry diagnosis.* Eur J Orthod. 1996; 18: 629–636

26. Proffit WR, Turvey TA. Dentofacial asymmetry. In: Proffit WR, White RP, Sarver DM editor. Contemporary Treatment of Dentofacial Asymmetry. St Louis: Mosby; 2003; p. 574–644.

27. Reyneke J, Tsakiris P, Kienle F*. A simple classification for surgical treatment planning of maxillomandibular asymmetry.* British Journal of Oral and Maxillofacial Surgery 1997; 35:349-351.

28. Richtsmeier J, Deleon V, Lele S. *The promise of geometric morphometrics.* Yearbook of Physical Anthropology 2002; 45: 63-91.

29. Sanders DA, Rigali PH, Neace WP, Uribe F, Nanda R. *Skeletal and dental asymmetries in Class II subdivision malocclusions using cone-beam computed tomography*. Am J Orthod Dentofacial Orthop. 2010 Nov; 138(5):542.e1-20; discussion 542-3.

30. Severt T, Proffit W. *The prevalence of facial asymmetry in the dentofacial deformities population at the University of North Carolina*. Int J Adult Orthodon Orthognath Surg 1997; 12: 171.

31. Shibata M, Nawa H, Kise Y, Fuyamada M, Yoshida K, Katsumata A, Ariji E, Goto S. *Reproducibility of three-dimensional coordinate systems based on craniofacial landmarks*. Angle Orthod 2012; 82:776-84.

32. Terajima M, Furuichi Y, Aoki Y, Goto T, Tokumori K, and Nakasima K. *A 3-dimensional method for analyzing facial soft-tissue morphology of patients with jaw deformities*. Am J Orthod Dentofacial Orthop 2009; 135:715-722.

33. Trpkova B, Prasad N, Lam E, Raboud D, Glover K, Major P. *Assesment of facial asymmetries from posteroanterior cephalograms: validy of reference lines*. Am J Orthod Dentofacial Orthop 2003; 123:512-520.

34. Van Valen L. *A study of fluctuating asymmetry*. Evolution 1962; 16: 125-142.

35. Vig P, Hewitt A. *Asymmetry of the Human Facial Skeleton*. The Angle Orthodontist 1975; 125-129.

36. Woo T. *On the asymmetry of the human skull*. Biometrika 1931; 22:324-341.

37. Yanez-Vico, R.M., et al., *Diagnostic of craniofacial asymmetry. Literature review*. Med Oral Patol Oral Cir Bucal 2010; 15: p. e494-8.
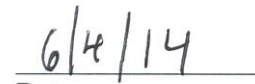
Publishing Agreement

It is the policy of the University to encourage the distribution of all theses, dissertations, and manuscripts. Copies of all UCSF theses, dissertations, and manuscripts will be routed to the library via the Graduate Division. The library will make all theses, dissertations, and manuscripts accessible to the public and will preserve these to the best of their abilities, in perpetuity.

Please sign the following statement:
I hereby grant permission to the Graduate Division of the University of California, San Francisco to release copies of my thesis, dissertation, or manuscript to the Campus Library to provide access and preservation, in whole or in part, in perpetuity.

_____   6/4/14
Author Signature   Date